RSC Advances

PAPER

View Article Online
View Journal | View Issue

Cite this: *RSC Adv.*, 2021, **11**, 21738

Ligand and adjuvant dual-assisted synthesis of highly luminescent and stable Cs_4PbBr_6 nanoparticles used in LEDs†

Zikuan Shi, ‡[a] Yu Yang,‡[a] Xin-Yuan Sun,[b] Feng Lang,[a] Yu Xiang[a] and Liangwu Lin*[a]

We developed a new ligand and adjuvant dual-assisted room temperature colloidal method for the synthesis of highly luminescent and stable Cs_4PbBr_6 nanoparticles, in which acetone, oleamine (OM) and oleic acid (OA) were used as precursors, while water and dimethyl sulfoxide (DMSO) were used as adjuvants. In this process, we explored the influencing factors of process parameters (such as the amount of water, the standing time of precursors, and the molar ratio of raw materials), and found that Cs_4PbBr_6 synthesized by water + DMSO can not only change the morphology and promote crystallization but also improve the lattice strain, reduce the lattice defects and optimize the passivation effect, so as to improve the luminescence properties. Simultaneously, we also found that the pc-LED made of Cs_4PbBr_6 can still emit bright green light after 4344 h of operation, showing excellent stability and making it promising for solid-state lighting application. This method also provides an important reference value for solving the hydrolysis property of perovskites.

Received 12th March 2021
Accepted 25th May 2021

DOI: 10.1039/d1ra01968f

rsc.li/rsc-advances

Introduction

Since the first report on all inorganic lead halide perovskite $CsPbBr_3$ in 2015,[1] it has attracted extensive attention at home and abroad due to its excellent luminescence and photoelectric properties, broad application prospects and simple preparation process.[2–4] Thereafter, research on $CsPbBr_3$ expanded rapidly. This development has also led to people's enthusiasm for other halogen perovskites (such as Cs_4PbBr_6 with zero dimensional structure).[5,6] Compared with $CsPbBr_3$, Cs_4PbBr_6 has better stability (such as moisture resistance, and heat resistance). Moreover, the mosaic structure of $CsPbBr_3/Cs_4PbBr_6$ composites can also improve it's optical properties and stability.[7] Therefore, this kind of perovskite materials have great research value.

In 2016, Cs_4PbBr_6 powders with strong and stable green photoluminescence (PL) were reported.[6,8] Soon after, the first reports on Cs_4PbBr_6 nanocrystals (NCs) emerged.[5,9] The most developed liquid-phase methods for the synthesis of Cs_4PbBr_6 NCs are the hot injection (HI) method[10,11] and the ligand-assisted re-precipitation (LARP) method.[12,13] In addition, this type of perovskite easily hydrolyzes and quenches the fluorescence when exposed to moist atmosphere, which is a topic that can never be ignored. However, a few reports on perovskite solar cells have shown improved performance in devices that have been exposed to moist atmosphere, either when synthesizing precursor solutions or during device fabrication.[14–18] Gong *et al.* investigated the influence of water additives on $CH_3NH_3PbI_{3-x}Cl_x$ perovskite thin films and the corresponding device performance. A small amount of water additive can enhance the crystallization, surface coverage, stability and conversion efficiency.[15] Zhang *et al.* showed that the water additive not only resulted in red-shifted PL peaks, higher PLQYs, and better crystallization of the $CsPbBr_3$ perovskite NCs, but also improved the device performance of LEDs based thereon.[18] Kim *et al.* reported that the controlled addition of water molecules in $CsPbBr_3$ NCs can encourage crystallization and strengthen the bonds between Pb and Br. Accordingly, water-assisted perovskite NCs demonstrate improved PLQY and stability.[16] $CsPbBr_3$ and Cs_4PbBr_6 crystals have been synthesized in DMSO, and they are often co-crystallized.[19–21] Moreover, the total coordination number of Pb(II) is around six in DMSO. Also, the structure of the intermediate (such as $PbBr_2 \cdot DMF$, $PbBr_2 \cdot DMSO$, and $PbBr_2 \cdot H_2O$) in solution plays a decisive role on the formation of perovskite product, and the Pb–O bond is replaced by Pb–Br gradually and the coordination number is maintained in the crystallization process.[22] Then, the DMSO induced transformation of the product to Cs_4PbBr_6 takes place.[23]

However, the role of water + DMSO for the synthesis and optical properties of Cs_4PbBr_6 is not reported. Here, we developed a new dual adjuvant-assisted room temperature colloidal

[a]*National Key Laboratory of Science and Technology on High-strength Structural Materials, Central South University, Changsha, Hunan 410083, People's Republic of China. E-mail: linliangwu@csu.edu.cn*

[b]*Department of Physics, Jinggangshan University, Ji'an, Jiangxi 343009, People's Republic of China*

† Electronic supplementary information (ESI) available: Experimental details and figures used in this work. See DOI: 10.1039/d1ra01968f

‡ Co first authors: Zikuan Shi, Yu Yang.

method (a modified LAPR method) for the synthesis of highly luminescence and stable Cs_4PbBr_6 nanoparticles makes it promising for the solid-state lighting application, in which acetone, oleamine (OM) and oleic acid (OA) were used as the precursor, and water and dimethyl sulfoxide (DMSO) as the adjuvant. Also, in the process, we also explored the influence mechanism of water and DMSO for the synthesis and optical properties of Cs_4PbBr_6 by changing the process parameters (such as the amount of water, the standing time of precursor, and the molar ratio of raw materials). This method also provides an important reference value for solving the hydrolysis property of the perovskite.

Experimental section

Materials

Cesium bromide (CsBr, 99.5% metals basis), lead(II) bromide ($PbBr_2$, AR, 99.0%), oleylamine (OM, 80–90%) and dimethyl sulfoxide (DMSO) were purchased from Aladdin. Ethyl acetate (EA), *n*-hexane (*n*-H), oleic acid (OA, AR), absolute ethanol and acetone were purchased from Sinopharm Chemical Reagent. All the reagents were used as received without any further purification.

Synthesis of Cs_4PbBr_6 nanocrystals

Cs_4PbBr_6 were synthesized at room temperature without any protective gas. 25 mL acetone was loaded into 150 mL conical flask at 25 °C. Subsequently, 5 mL OA and 2.5 mL OM were added into a conical flask with stirring for 1 min to homogenize it. After that the solid powders of 1 mmol $PbBr_2$ (0.367 g dissolved in 4 mL DMSO) and 1 mmol CsBr (0.213 g dissolved in deionized water) were added into the flask with vigorous stirring (1200 rpm) for 60 min. Successful synthesis of Cs_4PbBr_6 was proved by strong green fluorescence observed after irradiation by ultraviolet radiation. The crude solution was centrifuged at 7000 rpm for 5 min. Then, 10 mL acetone was added, followed by ultrasonic cleaning for 5 min and then centrifuged at 7000 rpm for 5 min. Finally, they were dried in a vacuum oven for 12 h at room temperature, and the obtained powder was characterized.

Characterization

X-ray diffractometry (XRD) patterns were collected on an X-ray automatic diffractometer (Advance D8, BRUGG GROUP, Switzerland) using Cu Kα radiation (wavelength = 1.55406 Å). The XRD pattern was recorded in the range of $10° \leq 2\theta \leq 60°$ at a scanning step of 0.02° and counting time 2s per step. Transmission electron microscopy (TEM) was carried out on a field emission scanning electron microscope (JEM-2100F, Japan). Photoluminescence (PL), photoluminescence excitation (PLE) spectra and time-resolved PL decay spectra were acquired on a full function fluorescence spectrometer (FLS-1000, Edinburgh, Britain). Ultraviolet and visible (UV-Vis) absorption spectra were measured with a UV-3600 Ultraviolet visible spectrophotometer (Shimadzu, Kyoto, Japan). X-ray photoelectron spectroscopy (XPS) was performed on a K-ALPHA X-ray photoelectron spectrometer (Thermo Fisher Scientific, Britain) in the 1300–0 eV region. Fourier transform infrared reflection (FTIR) spectra were obtained on a Nicolet instrument (iS5, Thermo, United States) in the region of 3800 to 400 cm^{-1}. Raman spectra were recorded on a Lab RAM HR800 spectrometer under exciting with a 633 nm laser light at room temperature, and recorded in the region of 50–500 cm^{-1}.

Results and discussion

In previous studies, water and dimethyl sulfoxide were used as the auxiliary agents to synthesize perovskites.[24] However, this method has an obvious disadvantage. The synthesized sample is easily dissolved in dimethyl sulfoxide shown in Fig. S1.† However, the perovskite samples can reappear by dropping acetone, which is caused by the solubility difference of perovskites in the two solutions. Therefore, we introduced the precursors (OM, OA, and acetone) in this method and carried out four groups of experiments: original, DMSO, water and water + DMSO (see Scheme 1). However, the perovskite could not be synthesized by adding DMSO only, as shown in Fig. S2.† The product had no fluorescence and was found to be cesium bromide as per XRD analysis. This may be due to the fact that cesium bromide cannot dissolve in acetone and DMSO, and it cannot reach the condition of ligand-assisted reprecipitation (LARP) method. Therefore, it will not be discussed below.

Fig. 1(a) and (b) show the digital optical photos of original Cs_4PbBr_6 samples as well as in water and water + DMSO under ambient light and under UV lamp. It can be seen clearly that the sample after adding water + DMSO (W + D) show obvious yellow green strong fluorescence, which is different from the other two samples. The fluorescence spectrum shows the fluorescence properties, as shown in Fig. 1(c) (exciton 360 nm). Compared with the original sample (peak: 530 nm), the addition of water (peak: 524 nm) results in blue-shift and the same change happens when W + D was added (peak: 516 nm). The above-mentioned data show that the addition of W + D can significantly improve the fluorescence intensity and FWHM (25.43 nm) of the perovskite samples. These results are considered likely to be the effects of reduced defect density that inhibits non-radiative recombination channels. Moisture such as water may improve the reconstruction process during the NC formation by partially dissolving the reactants and accelerating mass transport within NCs.[25] In Fig. 1(d), it can be seen that the absorption spectrum is composed of a sharp absorption peak at

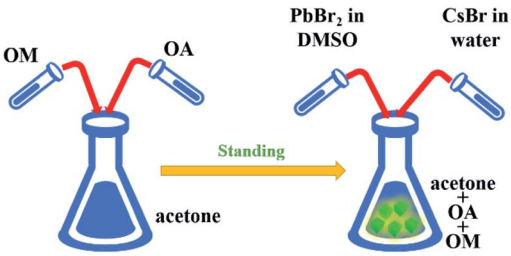

Scheme 1 The synthesis process of Cs_4PbBr_6.

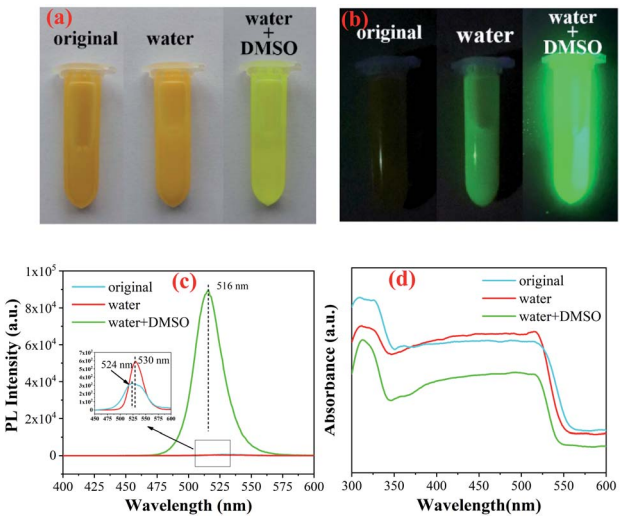

Fig. 1 The digital optical photos of Cs_4PbBr_6 samples of original, water and water + DMSO under ambient light (a) and under UV lamp (b); the photoluminescence emission (c) and absorption spectrum (d).

about 315 nm and a broad absorption band (320–550 nm). The strong absorption peak near 315 nm is related to Cs_4PbBr_6, originating from the optical transitions between the localized states within the isolated $PbBr_6^{4-}$ octahedra.[9,26] It has been reported that the absorption peak of pure $CsPbBr_3$ NCs is located at around 510 nm.[1,27] Therefore, it is reasonable to speculate that the absorption peak and strong PL peak near 520 nm in Fig. 1(d) originate from interfused $CsPbBr_3$ NCs.

Previous studies have shown that pure Cs_4PbBr_6 is an insulator with a large band gap of ~3.9 eV,[9,26,28] and $CsPbBr_3$ is a semiconductor with a band gap of about 2.3 eV.[29,30] The band-gap values (E_g) are obtained on the basis of the Tauc plot as the intercept value of the plot of $(\alpha h\nu)^{1/m}$ against light energy $h\nu$, where α is the absorption coefficient. It is found that m is equal to 1/2 for both $CsPbBr_3$ and Cs_4PbBr_6, indicating the feature of the direct-band-gap semiconductor, as shown in Fig. 2(a). For comparison, the band gap (E_{g_1}) of the samples were determined and found to be approximately 2.26 eV (original), 2.29 eV (water) and 2.30 eV (W + D), as shown in Fig. 2(b). The band gaps (E_{g_2}) of the samples were also determined and were found to be about 3.56 eV (original), 3.62 eV (water) and 3.63 eV (W + D) (see Fig. 2(c)). With the addition of water and W + D, the band gap increased evidently. These results indicate that a very small amount of water can enter the lattice of Cs_4PbBr_6 and lead to the formation of the hydroxyl sub-bandgap.[31] This result is in agreement with the PL spectra shown in Fig. 1(c). HRTEM was employed to investigate the microstructure of NCs. As shown in Fig. 2(d), the square NCs have uniform distribution and relatively uniform size (about 15 nm). The fast Fourier transformation (FFT) images inset at the right of the figure confirm that the monoclinic $CsPbBr_3$ and hexagonal Cs_4PbBr_6 exist together in the original sample. The d-spacing for two red fringes was measured to be 4.0 Å, which belongs to the (300) plane of hexagonal Cs_4PbBr_6 (JCPDS 74-2378). Further, the d-spacings for yellow fringes were measured to be 4.2 Å, 4.8 Å and 6.4 Å, belonging to the (022), (020) and (012) planes of monoclinic $CsPbBr_3$ (JCPDS 73-2463), respectively. After adding W + D, it can be seen clearly that $CsPbBr_3$ is embedded in Cs_4PbBr_6 and the orientation of the crystal plane changes, as shown in Fig. 2(e), which is similar to previous studies.[32] This may be due to the fact that water and DMSO fully occupy the vacancy of Pb ion in the synthesis process,[22] which makes Br ion easier to embed into the site and results in better crystallinity. In order to prove the universality of this method, we can also successfully synthesized the perovskite by replacing acetone in the precursor with ethanol and EA. Moreover, the results of XRD and SEM show that ethanol can not only promote the dissolution of CsBr (see Fig. S3†), but also etch, making the particle size smaller and more regular, as shown in Fig. S4.†

The crystal structure was determined by XRD. As shown in Fig. 3, the diffraction pattern clearly indicates that hexagonal Cs_4PbBr_6 (JCPDS 74-2378) was formed. However, there are too many starting materials in the original sample, and the reaction was not complete. In contrast, pure perovskite can be obtained by adding water or adding W + D, and there was no peak belonging to $CsPbBr_3$, the narrow and sharp peaks indicate the high crystallinity of the sample. The lattice strain is related to lattice defects and can be calculated *via* the Hall–Williamson method. The exact values for the lattice strain are also listed in Table 1. We found that the lattice strain of the original and the sample after the addition of water is one order of magnitude higher than that of the sample with W + D. This is corresponding to the luminous intensity of the photoluminescence emission spectrum (Fig. 1(c)), which provides evidence for the luminescence of the Cs_4PbBr_6 crystal structure. It illustrates that the addition of W + D can effectively improve the lattice integrity of the Cs_4PbBr_6 crystal.

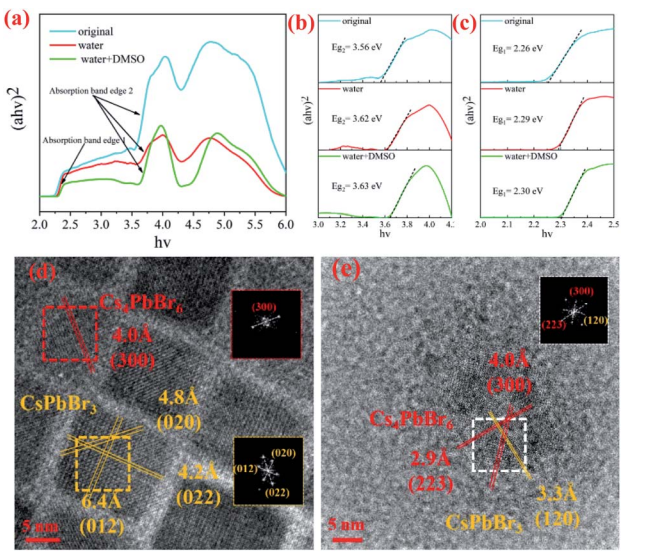

Fig. 2 The Tauc plot (a); local Tauc plot of the absorption band edge 1 (b) and edge 2 (c) for the absorption of sample original, water and water + DMSO; the high-resolution transmission electron microscopy (HRTEM) image of Cs_4PbBr_6 nanocrystalline synthesized by the original method (d) and W + D (e) (FFT corresponds to square selection).

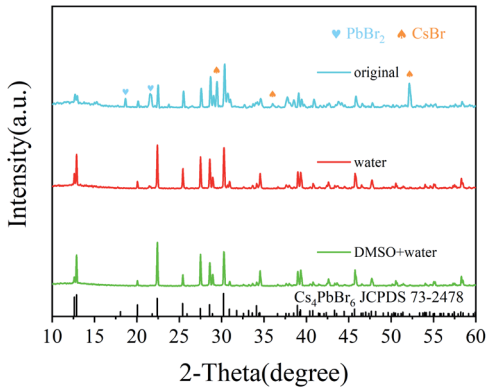

Fig. 3 The XRD patterns of sample original, water and W + D.

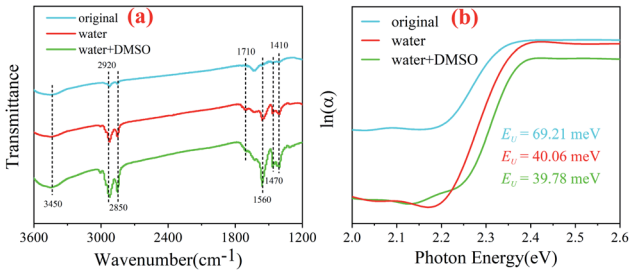

Fig. 4 The FTIR spectra of original, water and water + DMSO samples (a); logarithmic absorption coefficient of original, water and water + DMSO samples, as a function of photon energy (b).

OM and OA are usually used as surface ligands, playing a good passivation role during the synthesis process.[33–35] In order to explore the effects of water and dimethyl sulfoxide in this process, Fourier transform infrared reflection (FTIR) spectra of three samples are shown in Fig. 4(a). It can be seen that the peaks at 3450 cm^{-1}, 2930 cm^{-1}, 2850 cm^{-1}, 1710 cm^{-1}, 1560 cm^{-1}, 1470 cm^{-1} and 1410 cm^{-1} change in different degrees. The peak at 3450 cm^{-1} belongs to OH and a very small amount of water can enter the lattice of Cs_4PbBr_6 NCs due to the special structure of Cs_4PbBr_6. Simultaneously, OH are ionized and bound with matrix to form the hydroxyl sub-band gap.[31] Also, it can be seen from the figure that the peak intensity of the original and water sample is very weak, which may be due to the absorption of water in the air, but the W + D sample does have a significant enhancement, which indicates that there are some OH embedded in the Cs_4PbBr_6 lattice. The peak at 1710 cm^{-1} is due to the anti-symmetric stretching vibrations of C=O in COO^- owing to the existence of deprotonated COO groups; moreover, the peak at 1560 cm^{-1} is due to the symmetric bending vibrations of the protonated NH_3 groups, which can confirm the existence of the protonated oleylamine.[36] The peaks at 1470 cm^{-1} and 1410 cm^{-1} belong to C–N, which indicates that OA forms a primary amine salt with OM by donating its proton, leading to the formation of oleate, which then coordinates with Pb by partly replacing the bromide ion of $PbBr_2$ by the carboxylate group. Furthermore, according to the hard and soft acids and bases theory, Pb^{2+} is a borderline acid, whereas deprotonated OA and OM are both hard bases. Besides deprotonated OA and OM as a hard base can also readily coordinate with Pb.[37] Previous studies have shown that the coordination number of Pb^{2+} is six in the crystals produced from the solvents DMSO or DMF but becomes eight for H_2O as the solvent.[22] The water fully dissolves cesium bromide and DMSO can well combine with lead bromide to form a complex, which leads to the better coordination of the organic ligand with lead and plays a passivation role. The intensity change of the peaks (2930 cm^{-1} and 2850 cm^{-1}) belonging to $-CH_2$ and the peaks belonging to C–N also confirm this point.

In the synthesis process, different amounts of water significantly affect the luminescence properties and quantum lifetime of the samples, as shown in Fig. S5.† The introduction of appropriate amount of water can effectively increase the hydroxyl content in the precursor, thus improving the optical properties, which is consistent with the previous research results.[31] However, CsBr could not completely dissolve in less water and Cs_4PbBr_6 could not be synthesized in excess water (see Fig. S6†). Moreover, we found that standing time of the precursor has a great influence on the luminescence properties of the products, as shown in Fig. S7.† Among them, Cs_4PbBr_6 exhibited the best luminescence effects when allowed to stand for 6 h (Fig. S8†(a)), which may be attributed to the chain length of organic ligands. Previous studies have shown that long-chain surfactants can greatly improve the luminescence properties of the perovskite.[38] With the increase in the standing time, oleylamine and oleic acid condense to form long-chain ligands. After 6 h, water in the air continued to add in the reaction mixture which made the water content of the solution more, and the reaction proceeded in the opposite direction. In Fig. S7(b),† change of the amide bond (1620 cm^{-1}) strength provides a strong proof for the above-mentioned conclusion.

The absorption spectra were obtained to gain more insight into the degree of electronic disorder in the crystals, which is attributed to the fact that the absorption edge is known as the Urbach tail. The Urbach energy (E_U) reflects the cumulative effects of impurities, defects and electron–phonon interactions on NCs, which could be obtained by fitting the Urbach tails in the logarithmic absorption spectra according to the Urbach's rule:[39]

Table 1 The parameter and lattice strain of Cs_4PbBr_6

Sample	Emission peak (nm)	FWHM (nm)	E_{g_1} (eV)	E_{g_2} (eV)	Lattice strain (10^{-5})
Original	530	30.45	2.26	3.56	15.7
Water	524	49.08	2.29	3.62	30.0
Water + DMSO	516	25.43	2.30	3.63	1.41

$$\alpha(E) = \alpha_0 \exp\left(\frac{E - E_0}{E_U}\right) \quad (1)$$

$E_U = k_B T/\sigma(T)$ can be obtained, where k_B is the Boltzmann constant, T is the absolute temperature and σ is the steepness parameter.[40] Fig. 4(b) displays the E_U values of the nanocrystals synthesized in a mixture, which was obtained by fitting curves. It is observed that the E_U of the original sample is 69.21 meV, but it dropped sharply after the addition of water (40.06 meV) or W + D (39.78 meV). The nanocrystals with lower E_U indicates that they possess a lower degree of structural disorder and defect density than other nanocrystals.[41] This indicates that the solvents (water and W + D) are the key factors to control the internal defect density or structural disorder of nanocrystals during the synthesis process. Furthermore, some investigations proved that the Br^- concentration in the octahedron can be characterized by the red-shift of the absorption spectra.[42] Therefore, we can conclude that water or W + D may be useful to control the passivation effect on the nanocrystals, which is consistent with the FTIR analysis.

To study the chemical changes in Cs_4PbBr_6 synthesized by original and W + D methods, we conducted X-ray photoelectron spectroscopy (XPS). The full survey scan confirms the existence of Cs, Pb, Br in Cs_4PbBr_6, as shown in Fig. 5(a) and show strong peaks of Br (~68 eV), Pb (~138 and 143 eV) and Cs (~723 eV and 738 eV); these results agree with values in previous reports.[32,43,44]

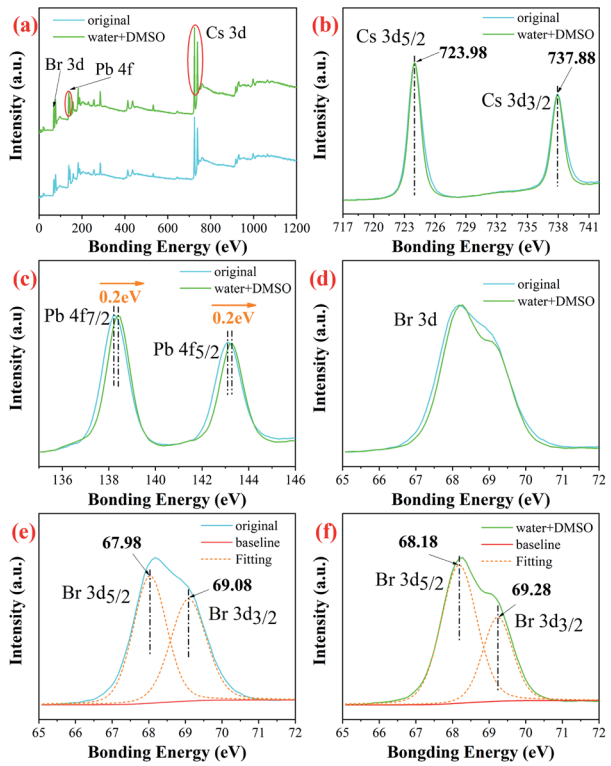

Fig. 5 Full survey scan of Cs_4PbBr_6 nanocrystals (a); high resolution XPS of (b) Cs 3d; (c) Pb 4f and (d) Br 3d; the fitted high resolution XPS of (e) and (f) Br 3d.

Table 2 The atomic percentage (%) of Cs_4PbBr_6 from XPS

Sample	Cs	Pb	Br	Cs : Pb : Br
Original	23	17	60	1.4 : 1 : 3.5
Water + DMSO	31	11	58	2.8 : 1 : 5.3

The high-resolution XPS spectra for the core level of Cs 3d, Pb 4f and Br 3d are given in Fig. 5(b) and (c). No obvious change was observed for the bonding energies of Cs 3d, as shown in Fig. 5(b). The peaks at 724.98 and 737.88 eV can be attributed to Cs $3d_{5/2}$ and Cs $3d_{3/2}$. The peak shapes of Pb 4f are similar for the two samples. However, the peak is shifted to a higher bonding energy for the W + D added sample, as shown in Fig. 5(c). In addition, the Br 3d peak can also be fitted into two peaks for Br $3d_{5/2}$ and Br $3d_{3/2}$, as shown in Fig. 5(d) and (f). Compared with the original sample, the W + D sample 0.2 eV blue-shift also occurs in Br 3d for the W + D added sample. The observed peak shift in Pb 4f and Br 3d spectra implies that strong bonds are formed between Pb and Br, and this strong interaction leads to the enhanced stability of Cs_4PbBr_6, occurring due to the removal of the surface defective layer.[45] Simultaneously, this phenomenon also indicates that the lattice composed of three elements (Cs, Pb, and Br) is more inclined to the standard lattice of 4 : 1 : 6, which indicates that the addition of W + D is helpful to decrease bromine vacancy and cesium vacancy. Table 2 provides strong evidence for this view. It can also be seen from the change of infrared peak intensity of water and W + D above (Fig. 4(a)). When the molar ratio of raw materials increases, the PL intensity of the as-synthesized Cs_4PbBr_6 will gradually decrease, which is similar to the previous study.[24] CsBr exists when the molar ratio exceeds 1 : 3, indicating that there was no complete reaction, as shown in Fig. S8.† The results of XPS (Fig. S9†) showed that the increase in the raw material ratio will lead to the shift of Cs and Br peaks to the left, indicating that the binding energy decreases and tends to be unstable.

Finally, pc-LED was fabricated by using a 365 nm near-UV LED chip and the synthesized Cs_4PbBr_6 (water + DMSO), and connected 3.0 volts to the two poles of the pc-LED shown in Fig. 6(a). To investigate the photo-bleaching stability of the as-

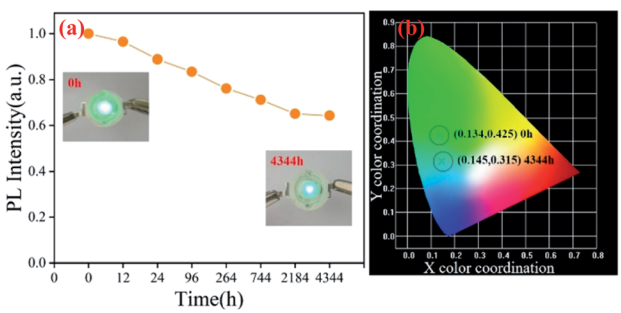

Fig. 6 The PL intensity of sample C under 365 nm near ultraviolet continuous irradiation (a); photographs and the positions in the CIE diagram for the pc-LEDs (b).

prepared phosphor under 365 nm, we used pc-LED to explore its photo-bleaching stability, as shown in Fig. 6(a). The results show that pc-LED can still emit green light normally after 4344 h, and the intensity is 62.3% of the initial PL intensity, which shows excellent photo-bleaching stability. Fig. 6(b) shows the photographs and the positions in the CIE diagram of pc-LEDs.

Conclusions

In summary, a new dual adjuvant-assisted room temperature colloidal method (a modified LAPR method) was developed for the synthesis of highly luminescent and stable Cs_4PbBr_6 nanoparticles using acetone, oleamine (OM) and oleic acid (OA) as the precursor, and water and DMSO as the adjuvant. In this process, we explored the influencing factors of process parameters (such as the amount of water, the standing time of precursor, and the molar ratio of raw materials), and found that Cs_4PbBr_6 synthesized by water + DMSO can not only change the morphology and promote crystallization but also improve the lattice strain, reduce the lattice defects and optimize the passivation effect, so as to improve the luminescence properties. Simultaneously, we also found that pc-LED made of the Cs_4PbBr_6 purified with acetone can emit green light even after 4344 h of operation, showing excellent stability and making it promising for the solid-state lighting application. This method also provides an important reference value for solving the hydrolysis property of perovskites.

Conflicts of interest

There are no conflicts to declare.

Acknowledgements

The authors are thankful for the financial support from the National Natural Science Foundation of China (Grant No. 31660266) and the Natural Science Foundation of Hunan Province, China (Grant No. 2018JJ2509).

Notes and references

1 L. Protesescu, S. Yakunin, M. I. Bodnarchuk, F. Krieg, R. Caputo, C. H. Hendon, R. X. Yang, A. Walsh and M. V. Kovalenko, *Nano Lett.*, 2015, **15**, 3692–3696.
2 X. Li, F. Cao, D. Yu, J. Chen, Z. Sun, Y. Shen, Y. Zhu, L. Wang, Y. Wei, Y. Wu and H. Zeng, *Small*, 2017, **13**, 1603996.
3 X. He, Y. Qiu and S. Yang, *Adv. Mater.*, 2017, **29**, 1700775.
4 M. V. Kovalenko, L. Protesescu and M. I. Bodnarchuk, *Science*, 2017, **358**, 745–750.
5 Y. Zhang, M. I. Saidaminov, I. Dursun, H. Yang, B. Murali, E. Alarousu, E. Yengel, B. A. Alshankiti, O. M. Bakr and O. F. Mohammed, *J. Phys. Chem. Lett.*, 2017, **8**, 961–965.
6 D. Chen, Z. Wan, X. Chen, Y. Yuan and J. Zhong, *J. Mater. Chem. C*, 2016, **4**, 10646–10653.
7 T. Xuan, S. Lou, J. Huang, L. Cao, X. Yang, H. Li and J. Wang, *Nanoscale*, 2018, **10**, 9840–9844.
8 M. I. Saidaminov, J. Almutlaq, S. Sarmah, I. Dursun, A. A. Zhumekenov, R. Begum, J. Pan, N. Cho, O. F. Mohammed and O. M. Bakr, *ACS Energy Lett.*, 2016, **1**, 840–845.
9 Q. A. Akkerman, S. Park, E. Radicchi, F. Nunzi, E. Mosconi, F. De Angelis, R. Brescia, P. Rastogi, M. Prato and L. Manna, *Nano Lett.*, 2017, **17**, 1924–1930.
10 G. Almeida, L. Goldoni, Q. Akkerman, Z. Dang, A. H. Khan, S. Marras, I. Moreels and L. Manna, *ACS Nano*, 2018, **12**, 1704–1711.
11 Q. Jing, Y. Xu, Y. Su, X. Xing and Z. Lu, *Nanoscale*, 2019, **11**, 1784–1789.
12 J. Zhang, A. Wang, L. Kong, L. Zhang and Z. Deng, *J. Alloys Compd.*, 2019, **797**, 1151–1156.
13 W. Li, W. Deng, X. Fan, F. Chun, M. Xie, C. Luo, S. Yang, H. Osman, C. Liu, X. Zheng and W. Yang, *Ceram. Int.*, 2018, **44**, 18123–18128.
14 P. Ramasamy, D.-H. Lim, B. Kim, S.-H. Lee, M.-S. Lee and J.-S. Lee, *Chem. Commun.*, 2016, **52**, 2067–2070.
15 X. Gong, M. Li, X.-B. Shi, H. Ma, Z.-K. Wang and L.-S. Liao, *Adv. Funct. Mater.*, 2015, **25**, 6671–6678.
16 M. Kim, J. H. Kim, M. Kim, C. S. Kim, J. W. Choi, K. Choi, J. H. Lee, J. Park, Y.-C. Kang, S.-H. Jin and M. Song, *J. Ind. Eng. Chem.*, 2020, **88**, 84–89.
17 G. E. Eperon, S. N. Habisreutinger, T. Leijtens, B. J. Bruijnaers, J. J. van Franeker, D. W. dequilettes, S. Pathak, R. J. Sutton, G. Grancini, D. S. Ginger, R. A. J. Janssen, A. Petrozza and H. J. Snaith, *ACS Nano*, 2015, **9**, 9380–9393.
18 X. Zhang, X. Bai, H. Wu, X. Zhang, C. Sun, Y. Zhang, W. Zhang, W. Zheng, W. W. Yu and A. L. Rogach, *Angew. Chem. Int. Ed.*, 2018, **57**, 3337–3342.
19 D. N. Dirin, I. Cherniukh, S. Yakunin, Y. Shynkarenko and M. V. Kovalenko, *Chem. Mater.*, 2016, **28**, 8470–8474.
20 J.-H. Cha, J. H. Han, W. Yin, C. Park, Y. Park, T. K. Ahn, J. H. Cho and D.-Y. Jung, *J. Phys. Chem. Lett.*, 2017, **8**, 565–570.
21 Y. Rakita, N. Kedem, S. Gupta, A. Sadhanala, V. Kalchenko, M. L. Bohm, M. Kulbak, R. H. Friend, D. Cahen and G. Hodes, *Cryst. Growth Des.*, 2016, **16**, 5717–5725.
22 M. Liu, J. Zhao, Z. Luo, Z. Sun, N. Pan, H. Ding and X. Wang, *Chem. Mater.*, 2018, **30**, 5846–5852.
23 B. Zhou, D. Ding, Y. Wang, S. Fang, Z. Liu, J. Tang, H. Li, H. Zhong, B. Tian and Y. Shi, *Adv. Opt. Mater.*, 2021, **9**, 2001435.
24 L. N. Quan, R. Quintero-Bermudez, O. Voznyy, G. Walters, A. Jain, J. Z. Fan, X. Zheng, Z. Yang and E. H. Sargent, *Adv. Mater.*, 2017, **29**, 1605945.
25 H. Zhou, Q. Chen, G. Li, S. Luo, T.-b. Song, H.-S. Duan, Z. Hong, J. You, Y. Liu and Y. Yang, *Science*, 2014, **345**, 542–546.
26 M. Nikl, E. Mihokova, K. Nitsch, F. Somma, C. Giampaolo, G. P. Pazzi, P. Fabeni and S. Zazubovich, *Chem. Phys. Lett.*, 1999, **306**, 280–284.
27 X. Li, Y. Wu, S. Zhang, B. Cai, Y. Gu, J. Song and H. Zeng, *Adv. Funct. Mater.*, 2016, **26**, 2435–2445.

28 M. Hu, C. Ge, J. Yu and J. Feng, *J. Phys. Chem. C*, 2017, **121**, 27053–27058.
29 S. Ananthakumar, J. R. Kumar and S. M. Babu, *J. Photon. Energy*, 2016, **6**, 042001.
30 K. Lin, J. Xing, L. N. Quan, F. P. G. de Arquer, X. Gong, J. Lu, L. Xie, W. Zhao, D. Zhang, C. Yan, W. Li, X. Liu, Y. Lu, J. Kirman, E. H. Sargent, Q. Xiong and Z. Wei, *Nature*, 2018, **562**, 245–248.
31 X. Wang, J. Yu, M. Hu, Y. Wu, L. Yang, W. Ye and X. Yu, *J. Lumin.*, 2020, **221**, 116986.
32 X. Chen, F. Zhang, Y. Ge, L. Shi, S. Huang, J. Tang, Z. Lv, L. Zhang, B. Zou and H. Zhong, *Adv. Funct. Mater.*, 2018, **28**, 1706567.
33 M. A. Uddin, J. K. Mobley, A. A. Masud, T. Liu, R. L. Calabro, D.-Y. Kim, C. I. Richards and K. R. Graham, *J. Phys. Chem. C*, 2019, **123**, 18103–18112.
34 T. Udayabhaskararao, L. Houben, H. Cohen, M. Menahem, I. Pinkas, L. Avram, T. Wolf, A. Teitelboim, M. Leskes, O. Yaffe, D. Oron and M. Kazes, *Chem. Mater.*, 2018, **30**, 84–93.
35 Q. Dai, S. Maloney, W. Chen, U. Poudyal and W. Wang, *Nanotechnology*, 2016, **27**, 225401.
36 Y. Liu, M. Guo, S. Dong, X. Jiao, T. Wang and D. Chen, *J. Mater. Chem. C*, 2018, **6**, 7797–7802.
37 H. Huang, J. Raith, S. V. Kershaw, S. Kalytchuk, O. Tomanec, L. Jing, A. S. Susha, R. Zboril and A. L. Rogach, *Nat. Commun.*, 2017, **8**, 996.
38 Y. Yuan, Z. Liu, Z. Liu, L. Peng, Y. Li and A. Tang, *Appl. Surf. Sci.*, 2017, **405**, 280–288.
39 S. M. Wasim, G. Marin, C. Rincon, P. Bocaranda and G. S. Perez, *J. Phys. Chem. Solids*, 2000, **61**, 669–673.
40 R. C. Rai, *J. Appl. Phys.*, 2013, **113**, 153508.
41 F. Liu, Y. Zhang, C. Ding, S. Kobayashi, T. Izuishi, N. Nakazawa, T. Toyoda, T. Ohta, S. Hayase, T. Minemoto, K. Yoshino, S. Dai and Q. Shen, *ACS Nano*, 2017, **11**, 10373–10383.
42 D. Yang, X. Li, Y. Wu, C. Wei, Z. Qin, C. Zhang, Z. Sun, Y. Li, Y. Wang and H. Zeng, *Adv. Opt. Mater.*, 2019, **7**, 1900276.
43 X. Wei, J. Liu, H. Liu, X. Le, H. Qian, H. Zeng, F. Meng and W. Deng, *Inorg. Chem.*, 2019, **58**, 10620–10624.
44 P. Uthirakumar, H. Yun, M. Devendiran, W. W. Lee and I.-H. Lee, *J. Lumin.*, 2019, **209**, 163–169.
45 J. Endres, M. Kulbak, L. Zhao, B. P. Rand, D. Cahen, G. Hodes and A. Kahn, *J. Appl. Phys.*, 2017, **121**, 035304.